Chapter 5
Blood Flow in Arteries and Veins

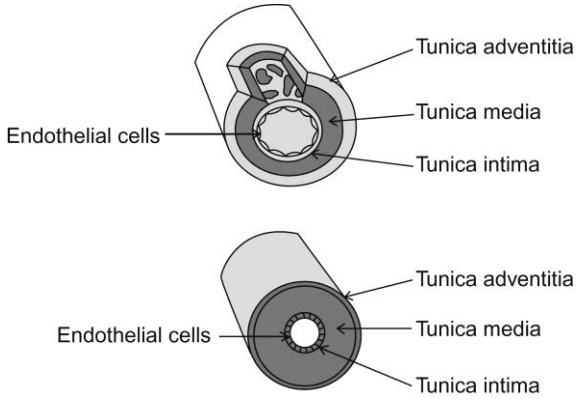

Figure 5.1 Anatomical structure of large elastic arteries and muscular arteries, respectively. In both of these types of blood vessels, the tunica media, which is composed of smooth muscle cells, is thick to withstand the high pressures within the arterial system. The tunica adventitia is composed of elastic fibers and helps to anchor the blood vessel to the surrounding tissue. The internal layer, the tunica intima, is composed of endothelial cells that are in contact with blood.

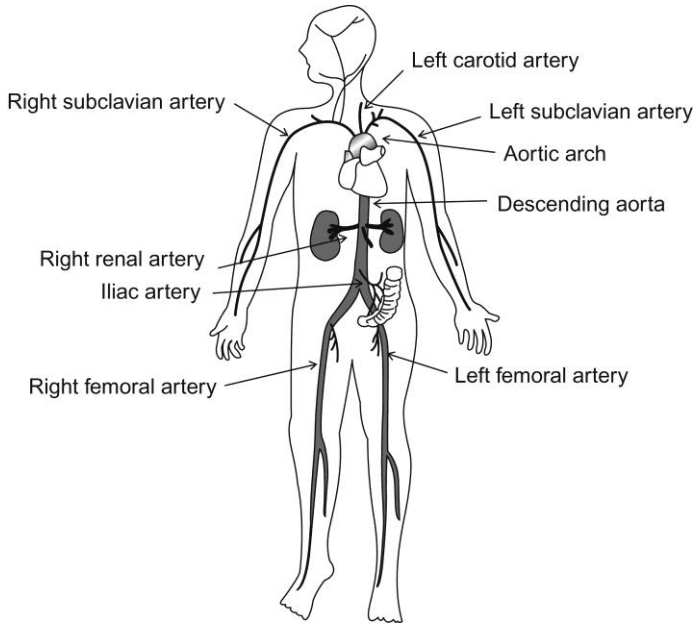

Figure 5.2 A schematic of the major arteries within the systemic circulation. After passing from the heart, into the aorta, oxygenated blood can enter the carotid arteries (feed the head), the subclavian arteries (feed the arms), the renal arteries (feed the kidneys), the iliac arteries (feed the pelvic region), or the femoral arteries (feed the lower limbs). There are other vessels that branch off the aorta that are not included within this figure.

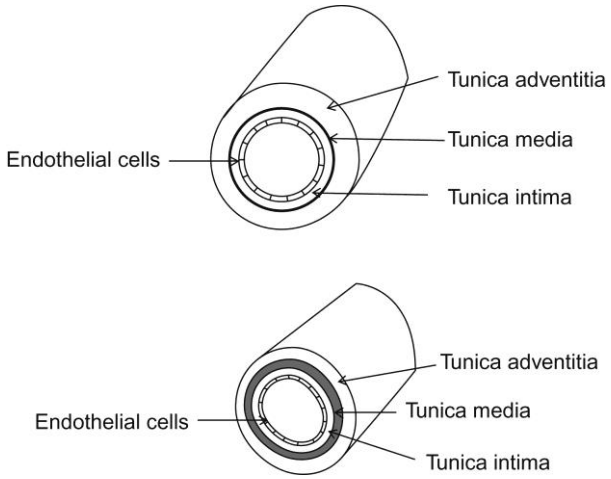

Figure 5.3 Anatomical structure of large elastic veins and medium-sized veins, respectively. The tunica adventitia is composed of elastic fibers and helps to anchor the blood vessel to the surrounding tissue. This is the thickest layer in veins. The tunica media is composed of smooth muscle cells and is smaller in veins as compared to arteries because they are under a lower pressure. The internal layer, the tunica intima, is composed of endothelial cells that are in contact with blood.

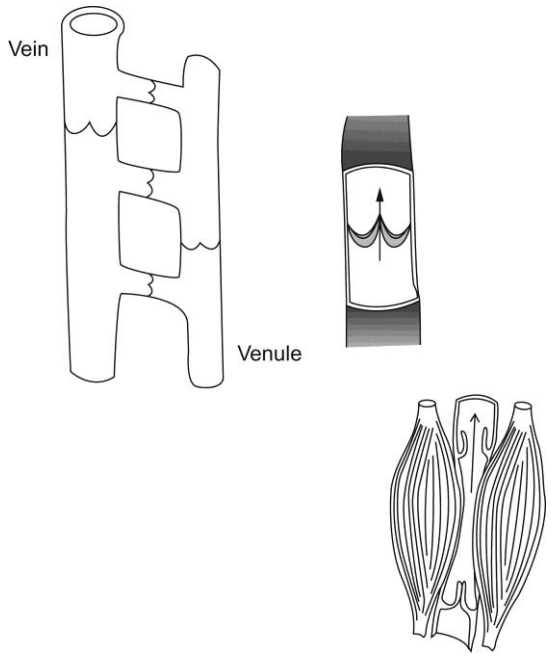

Figure 5.4 Venous valves determine the direction of blood within the venous system, preventing blood flow back toward the capillaries. Skeletal muscle contraction helps to transiently increase the pressure within veins to propel blood toward the heart. Arrows depict blood flow direction. The venous valve system is useful in the lower extremities when blood pressure cannot overcome the hydrostatic pressure.

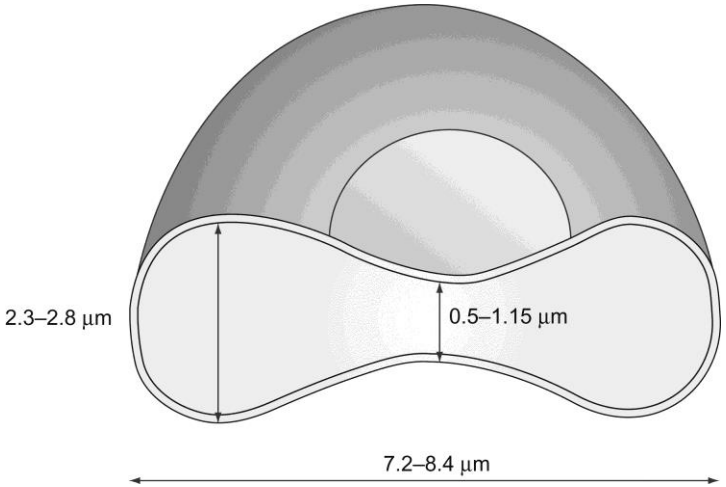

Figure 5.5 Cross-sectional view of a mature red blood cell. We also include the average range for various dimensions of a mature red blood cell. Each red blood cell contains hemoglobin molecules that facilitate the transport of oxygen and carbon dioxide throughout the cardiovascular system. There are approximately 5,000,000 red blood cells/μL of blood, and each red blood cell remains in circulation for approximately 120 days.

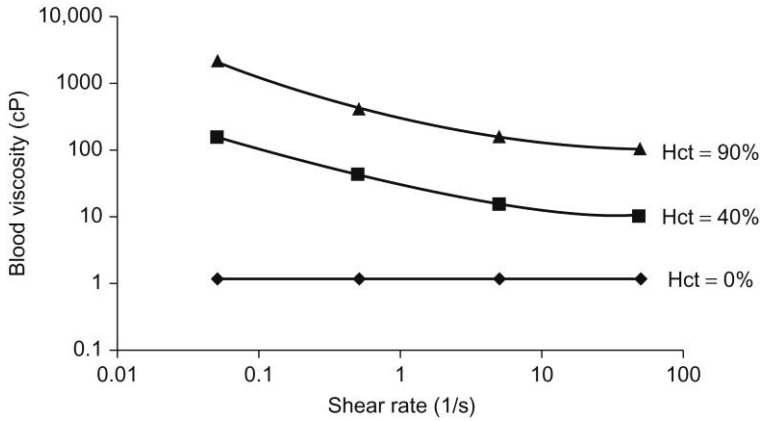

Figure 5.6 The variation in blood viscosity as a function of shear rate and blood hematocrit (Hct). This figure illustrates that without the cellular component the blood viscosity remains constant, at approximately 1.2 cP, over the range of shear rates depicted on the figure. When cells are present in the blood, the viscosity is no longer constant and increases with decreasing shear rate. This figure is a summary of data collected by Chien et al.

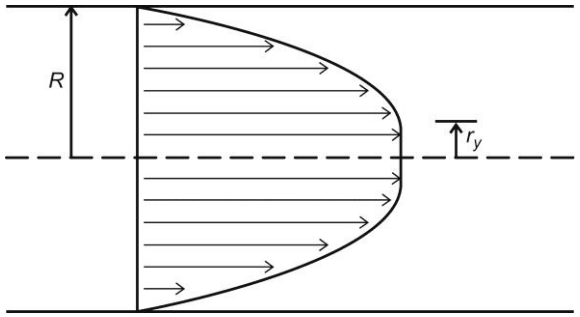

Figure 5.7 The velocity profile of blood flowing through a cylindrical vessel using the Casson model. The profile is blunter than a purely Newtonian fluid's velocity profile because the fluid that is between the centerline and r_y flows as a solid. At r_y, the shear stress surpasses the yield stress of the fluid (τ_y) and the viscous forces take effect.

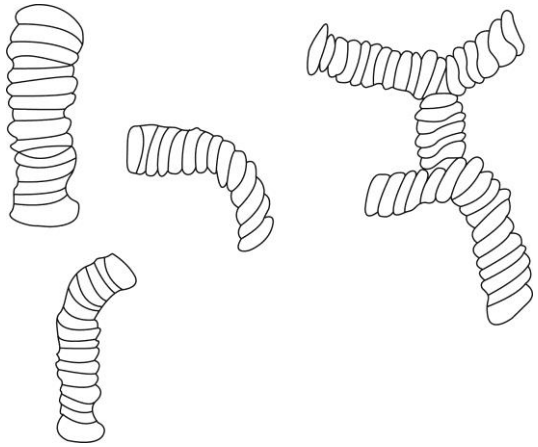

Figure 5.8 Red blood cell aggregates termed rouleaux, which can form linear or branched structures. The number of red blood cells in a rouleaux can vary from 2 to approximately 50. Red blood cells in the microcirculation typically traverse through capillaries within rouleaux structures.

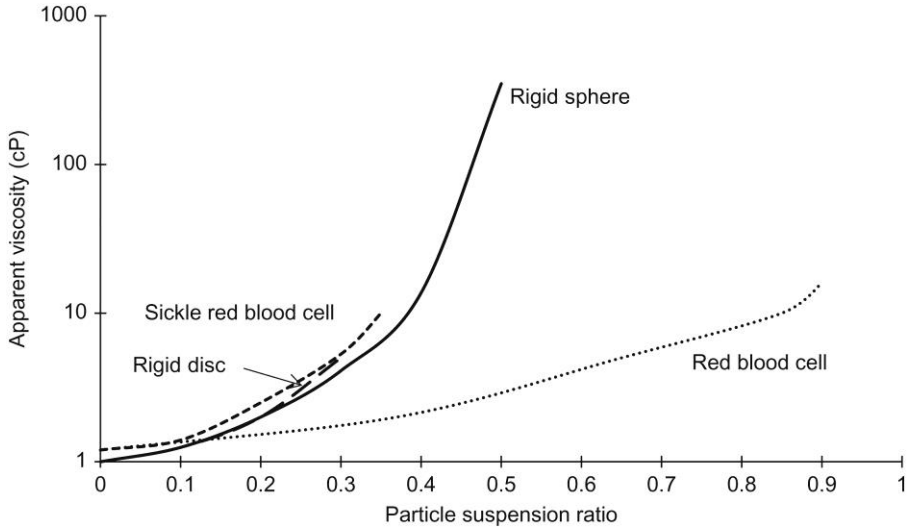

Figure 5.9 Investigations to determine the apparent viscosity of a suspension at a given shear rate. It has been shown that as the particle suspension ratio (e.g., the hematocrit for blood) increases, the apparent viscosity of the solution also increases. Investigations into the mechanical properties of the red cell membrane have shown that the fluid properties of the membrane prevent a massive increase in apparent viscosity, with marginal increase in particle suspension ratio. Rigid spheres or rigid discs, with a similar size/area as red blood cells show this large increase in apparent viscosity with small changes in suspension ratio. Additionally, sickle red cells lose their fluid-like properties

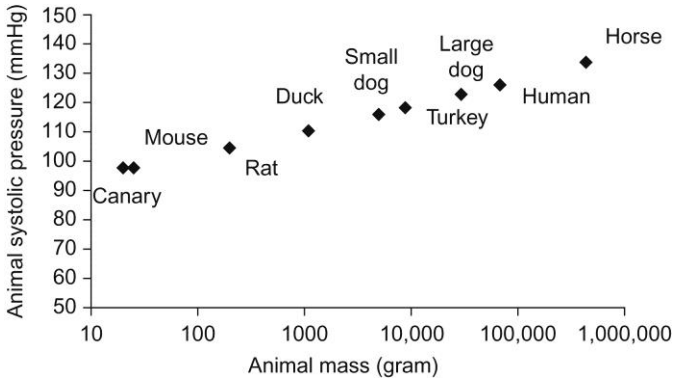

Figure 5.10 The relationship between animal mass and mean systolic pressure. As the mass of the animal increases, there is a general increase in systolic pressure. The relationship between these two measurements can be correlated to many different properties of the animal, as described in the text.

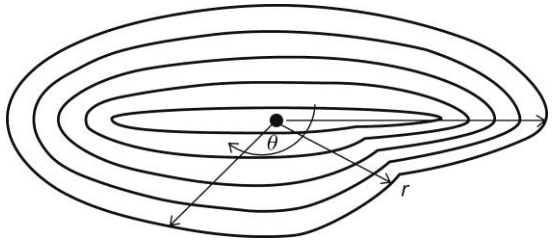

Figure 5.11 Schematic of a vein with a nonstandard geometry, shown by varying radial's length at various angles, θ. The method of choosing laminas of known average velocities still apply to these vessels; however, one would need to take account for the different areas of each lamina. Additionally, one would need to consider whether or not the fluid properties change as a function of the different radial directions.

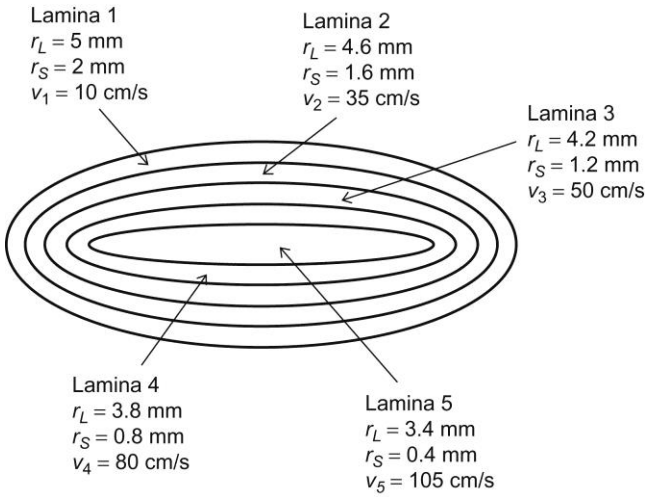

Figure 5.12 Figure associated with example problem.

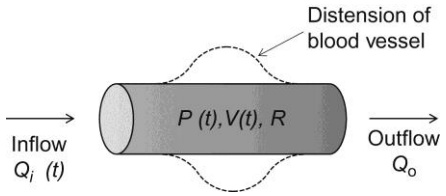

Figure 5.13 Schematic of a distensible arterial tree which can accommodate increases in blood flow via an increased volume. If we assume that the outflow flow rate has little variation in time, then we can analyze this type of vessel using a Windkessel approach as outlined in the text.

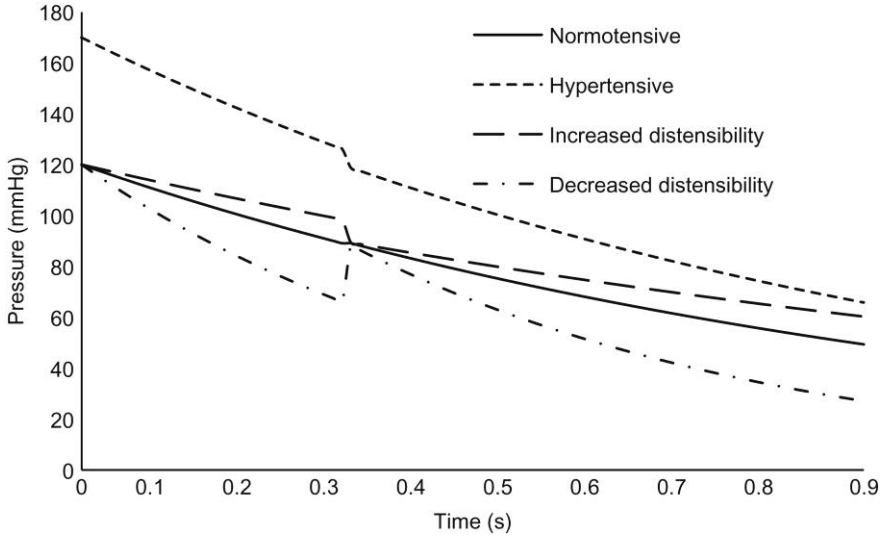

Figure 5.14 Figure associated with the example problem. Note that the pressure values were set to P_S = 120 mmHg and P_D = 80 mmHg for all cases, except the hypertensive case (P_S = 170 mmHg and P_D = 120 mmHg). The distensibility was either increased or decreased by 50% to arrive at the other curves.

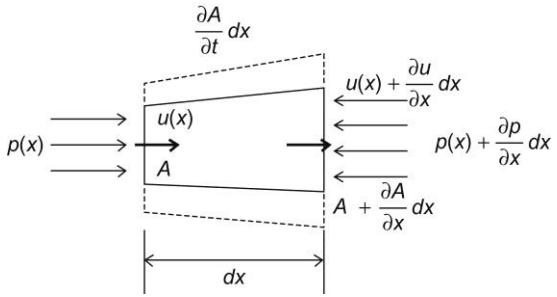

Figure 5.15 Wave propagation within a deformable homogenous artery. With a deformable boundary, one would need to take into account the change in area, with time, of the fluid element. The material properties of the arterial wall need to be included within this formulation as well.

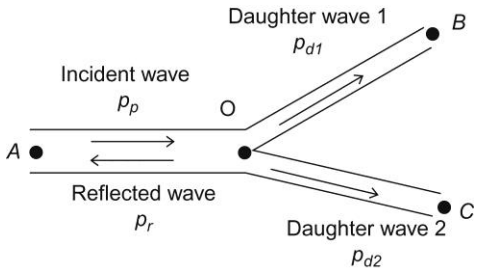

Figure 5.16 Pressure wave reflectance and transmittance at a bifurcation. The pressure pulse is reflected back along the mother branch, but this is normally out of phase with the next incident wave and therefore the entire pressure would be reduced. The energy of the transmitted waves do not summate to the energy of the incident wave.

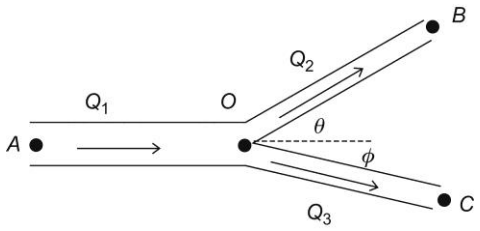

Figure 5.17 Flow rate at a bifurcation would be divided into two daughter branches. The geometry (angles and radii) of the bifurcation determines the division of the flow within the two daughter branches. By assuming that the work of supplying tissue with oxygen for each vessel should be minimized, one can derive a relationship between the vessels.

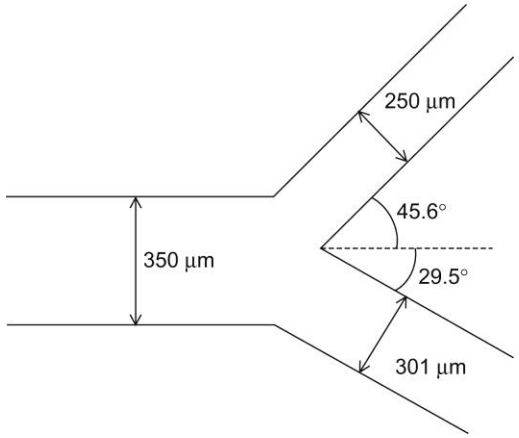

Figure 5.18 Schematic of the bifurcation found in the sample problem.

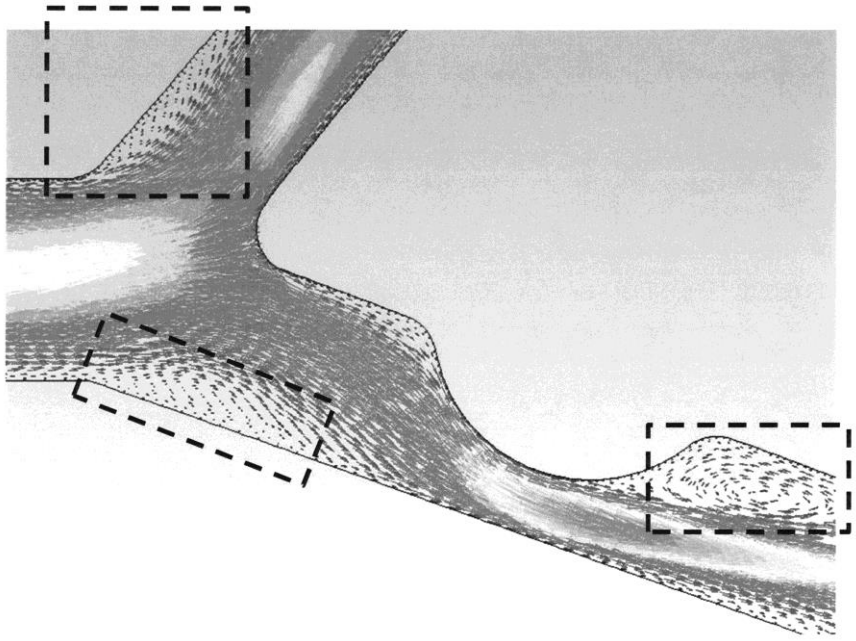

Figure 5.19 Flow separation (region enclosed by dashed lines) downstream of a bifurcation and a stenosis (rapid area expansions). Flow separates from the wall partially due to the skewing of the velocity profile toward one of the walls of the blood vessel. By quantifying the pressure gradient along the wall, the likelihood for flow separation can be predicted.

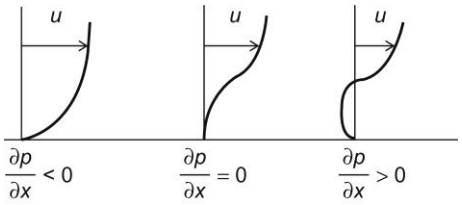

Figure 5.20 Effects of a pressure gradient on the flow profile near the wall. With an adverse (or positive) pressure gradient along the wall, the flow would tend to separate. With a negative or zero wall pressure gradient, the flow would not likely separate.

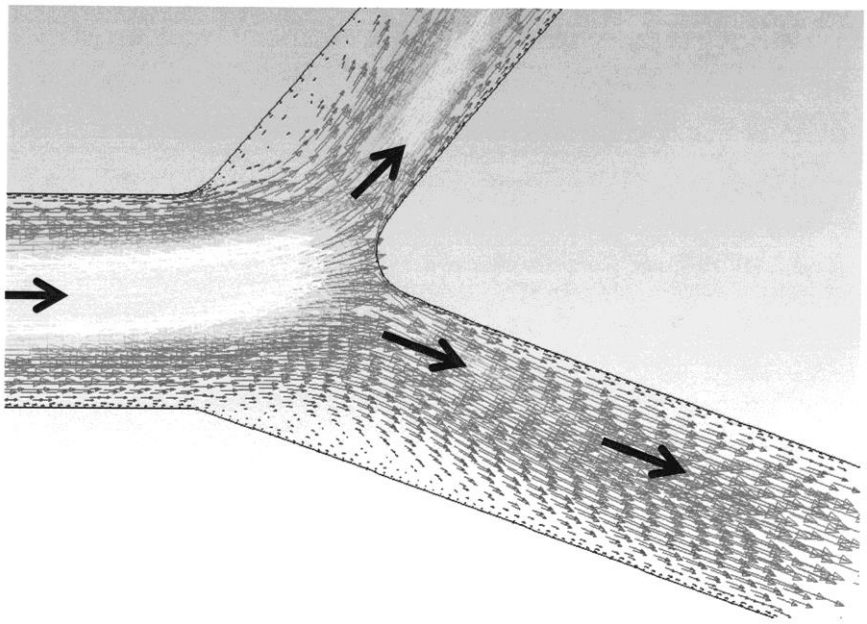

Figure 5.21 Flow skew at a bifurcation, where the highest velocity blood flow is no longer at the centerline (highest velocity is marked by black arrows). The extent of flow skewing is determined by the geometry of the bifurcation.

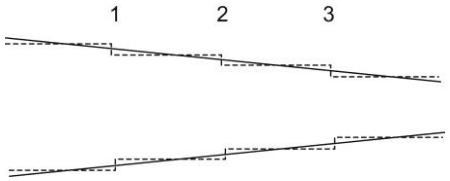

Figure 5.22 The modeling of a continuous taper with evenly spaced steps. To calculate the velocity profile through a continuous taper, one would need to determine the exact taper function, which may not be as simple as the examples shown in the text. However, if the taper is complicated, it can be approximated with discrete steps.

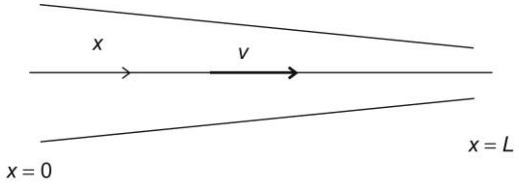

Figure 5.23 Model of a continuous taper for the example problem.

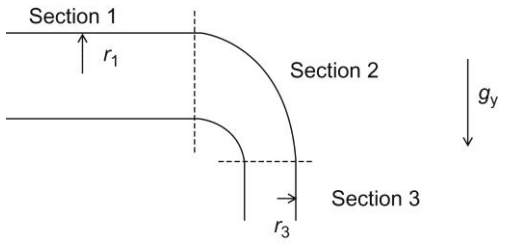

Figure 5.24 Cross-section of a tapered curving blood vessel. This problem shows the difficulty of adding a tapering blood vessel with changes in orientation.

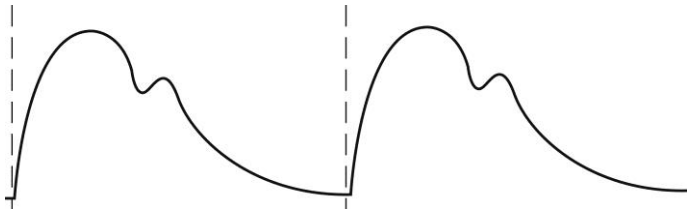

Figure 5.25 A schematic of the velocity waveform in a large artery, such as the aorta, showing that the velocity changes temporally and is pulsatile. As we can see, this mimics the pressure pulse of the left ventricle, but is reasonably constant with time.

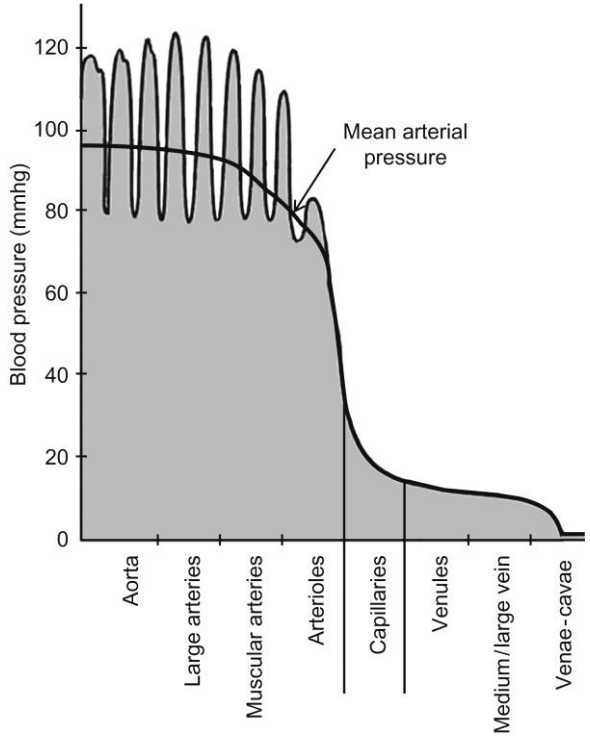

Figure 5.26 Pressure variation within the systemic circulation, illustrating that (i) there is a variation in pressure spatially along the systemic circulation and (ii) that within a specific level within the systemic circulation, the pressure varies with the systolic and diastolic contractions of the heart. The mean arterial pressure is the effective pressure in the systemic circulation.

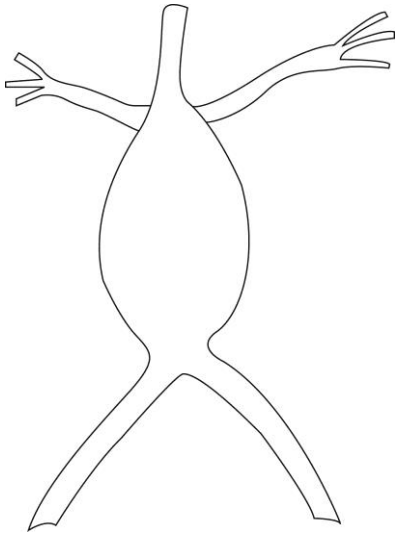

Figure 5.27 Schematic of a saccular aortic aneurysm, which is a bulging of the blood vessel wall. Normally, the wall bulges because there is a deterioration of the muscular mass in the wall and due to the constant pressure loading the wall begins to bulge. In severe cases, the wall can deteriorate to such an extent that the vessel breaks and blood begins to pool in the extravascular space.

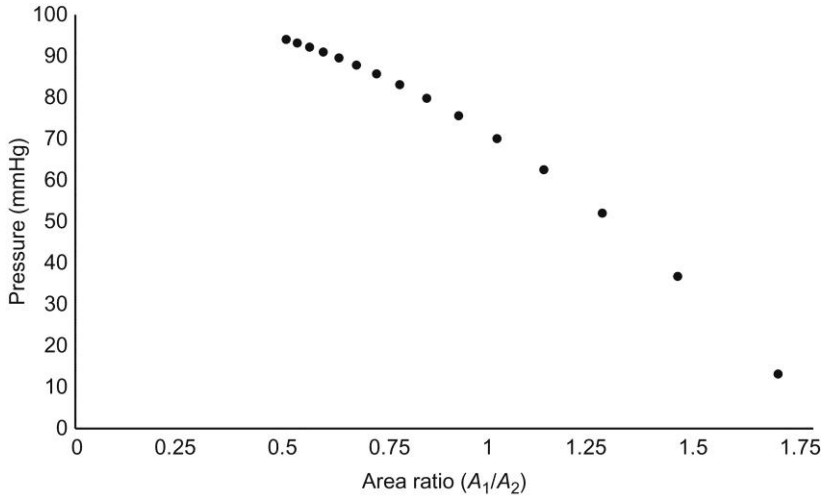

Figure 5.28 Relationship between the ratio of the inlet area (A_1) to the outlet area (A_2) and the pressure recorded at the outlet area. This assumes that there is no variation within height, viscous dissipation can be ignored and that there are no temporally varying components to this flow. As the ratio increases (as would be seen during a stenosis), the pressure decreases and as the ratio decreases (as would be seen during an aneurysm), the pressure increases.

.